JOURNAL OF SOLID STATE CHEMISTRY 104, 6–20 (1993)

A Computational Study of the Energetics and Lattice Dynamics of Germanium Containing Zeolitic Solids

A. R. GEORGE, C. R. A. CATLOW, AND J. M. THOMAS

Davy Faraday Laboratory, The Royal Institution of Great Britain, 21 Albemarle St., London, W1X 4BS, United Kingdom

Received October 29, 1992; accepted November 9, 1992

Lattice energy minimization techniques have been used to predict the stability of germanium analogues of common zeolite structures. The calculations suggest that complete solid solutions may occur for SiO_2 and GeO_2 in the quartz, mordenite, silicalite-I, and zeolite-Y structures, with only small deviations from ideality and lattice parameter variations consistent with Vegard's law. Nonrandom distributions of Si and Ge over tetrahedral (T) sites, however, lead to deviations from the predicted linearity of the variations of the lattice parameter with composition. Calculated infrared spectra are also presented for the four structures with varying Si : Ge ratios. Again, it is predicted that with nonrandom Si/Ge distributions, there are substantial changes in the calculated vibrational spectra.

Introduction

The quest for new types of microporous, microcrystalline solids continues unabated. To the substantial number of naturally occurring (aluminosilicate) zeolites, a variety of new zeolitic aluminosilicates, having structures not yet found in nature, have been added during the past 40 years (*1*). Great strides have also been made in producing families of microporous aluminophosphates (ALPOs), of whose structures some are unique and some are exactly akin in a framework structural sense to those of natural and synthetic zeolites (*2, 3*). In addition, many ALPO structures have been synthesized (*4, 5*) in which a transition metal or main-group metal has been inserted into the framework structure. And very recently, quite stable as well as unstable microporous structures containing germanium as the tetrahedrally coordinated atom have been synthesized.

Although it has not yet proved possible to prepare a range of germanium-based microporous structures comparable to those of the siliceous extremes of the well-known pentasils (epitomized by silicalite-I, the SiO_2 extreme of ZSM5, and by silicalite-II, the corresponding extreme of ZSM11), or indeed of mordenite and other important zeolites, considerable insight may be gained into the theoretical possibility of the existence of such materials by computational analysis of the kind we describe below. As well as arriving at the energetics of the germanate analogues of the (alumino)silicate zeolites, we can also predict the vibrational frequencies of the local and extended modes of these "computationally created" structures.

In this paper we investigate several structures, ranging from quartz to mordenite to zeolite-Y and finally to the large unit cell

0022-4596/93 $5.00

structure of silicalite-I. Mordenite is especially interesting since it has four distinct tetrahedrally coordinated crystallographic sites and it presents an ideal example where the effect of substitution at each site can be investigated. Various mole fractions (ranging from zero, i.e., purely siliceous, to unity, i.e., purely germanic) of Ge have been used in the modeling procedure. The spatial arrangement of the substituted ions (Ge^{4+} for Si^{4+}) is also varied between a variety of ordered models on the one hand and arrangements that are as nearly as possible random (within the constraints of the periodic boundary conditions technique used in this study) on the other. The techniques employed in our investigation are described in greater detail in the next section.

Computational Method

Lattice energy minimization calculations were performed on each system, using shell model potentials (*6*) which describe polarization effects simply and reliably. Potentials for aluminosilicates are readily available (*7*). Details are given in the Appendix. Parameters have recently been developed for the Ge—O interaction using an empirical fitting procedure by Bell (*8*). Again details are reported in the Appendix. The lattice energy calculations employ the now standard summation procedures for the short range and coulombic interactions, with the latter evaluated using the Ewald (*9*) technique. These summation procedures embody the two-body and three-body interatomic potential approximation, and can be quantified by the following equation:

$$v = \frac{1}{2}\sum_i \left(\sum_{j \neq i} \frac{q_i q_j}{r_{ij}} + \sum_{j \neq i} \left[A_{ij} \exp\left\{ \frac{-r_{ij}}{p_{ij}} \right\} - \frac{C_{ij}}{r_{ij}^6} \right] + \sum_{j \neq i, l \neq \{i,j\}} k_{ijl} [\vartheta_{ijl} - \vartheta_{ijl}^O]^2 \right)$$

v = Potential energy.
q_i = Charge of atom i.
r_{ij} = Distance between atoms i and j.
A_{ij}, p_{ij}, C_{ij} = Parameters of the Buckingham term.
ϑ_{ijl} = Angle between bonds ij and il.
ϑ_{ijl}^O = Equilibrium angle between bond ij and il.
k_{ijl} = Three-body force constant.

Full energy minimization is undertaken with respect to both cell dimensions and atomic coordinates. The THBREL (*10*) code was used for all the lattice simulations and embodies the equations reported above, coupled with a Newton–Raphson minimization procedure.

The generation of the predicted spectra is performed using the relaxed structure and the corresponding interatomic potentials. We employ standard lattice dynamical theory based on the harmonic approximation (which has been extensively applied to silicates by Parker and Price (*11*)). The calculations use the THBPHON (*12*) code, which generates both the frequencies and the atomic displacement vectors of the vibrational modes by diagonalizing the dynamical matrix of the system, without any use of the symmetry properties. The infrared (IR) and Raman spectra can be derived from the vibrational modes by dividing the modes into infrared active, Raman active, and inactive modes using group theoretical projection methods (*13*). The position of the spectroscopic lines can then be calculated, while the IR line intensities are evaluated using the method of Kleinman and Spitzer (*14*). As argued in Ref. (*15*), the spectrum obtained can be made more directly comparable with experiment by fitting a Gaussian curve (*16*), with a half width of 10 cm^{-1}, to each peak.

Results and Discussion

Part 1. Properties Related to the Energetics of the Structure

For each system we present results for both the structure and energetics as a function of composition. In the former case the lattice parameters are given, while in the latter we report heats of mixing, U_{mix}, calculated from the expression

$$U_{\text{mix energy}} = U_{\text{calc}}(x) - xU_{\text{Pure GeO}_2} - [1 - x]U_{\text{Pure SiO}_2},$$

where $U_{\text{calc}}(x)$ is the calculated lattice energy of the mixed system with mole fraction x of Ge, and U_{GeO_2} and U_{SiO_2} are the lattice energies of GeO_2 and SiO_2, respectively. The results for each structure are given below.

Quartz structure. This structure has three tetrahedral atoms in the asymmetric unit cell, thus restricting the possible range of substitutions by Ge ions when one only one unit cell is considered. When a supercell is used, there is, however, a considerable increase in the possible substitutional arrangements. As can be seen in Fig. 1, there is a linear relationship between the energy and the mole fraction of Ge, suggesting that the system is close to an ideal solution. This

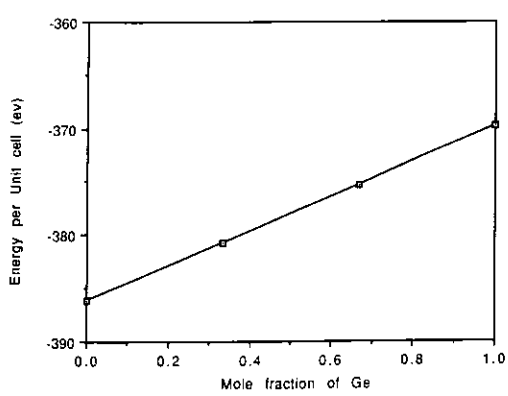

FIG. 1. Energy of the unit cell vs the mole fraction of Ge.

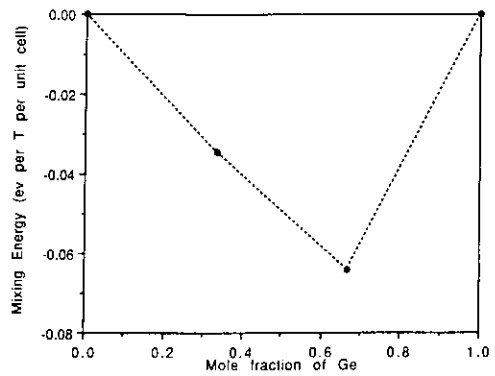

FIG. 2. The mixing energy of a quartz type structure vs mole fraction Ge.

conclusion is reinforced by Fig. 2, which shows the variation in the mixing energy (in eV per tetrahedral atom per unit cell) against mole fraction. The lowest energy ratio of Ge to Si is at this point, where the Ge/Si ratio is close to unity. The heats of mixing of only approximately 4 KJ/mole indicate only small deviations from ideality. Figure 3(a,b,c) describes the variation of the cell parameter with the mole fraction of substituted Ge. These graphs show a distinct if modest deviation from the linear relationship observed in the energy plot. The deviation is of the order of $+5\%$ in the a and b directions and $\pm 5.5\%$ in the c direction from the cell parameters of the purely siliceous form. Nevertheless, such deviations are largely attributable to the small unit cell employed in the simulation and our overall conclusion is that the SiO_2/GeO_2 system is close to ideality, with complete solid solubility.

The only data with which direct comparison can be made concerns the pure GeO_2 system (17,21) for which we overestimate the a/b lattice parameter by approximately 1.7% (see Table I), whereas Ge—O bond lengths are underestimated by approximately 3%.

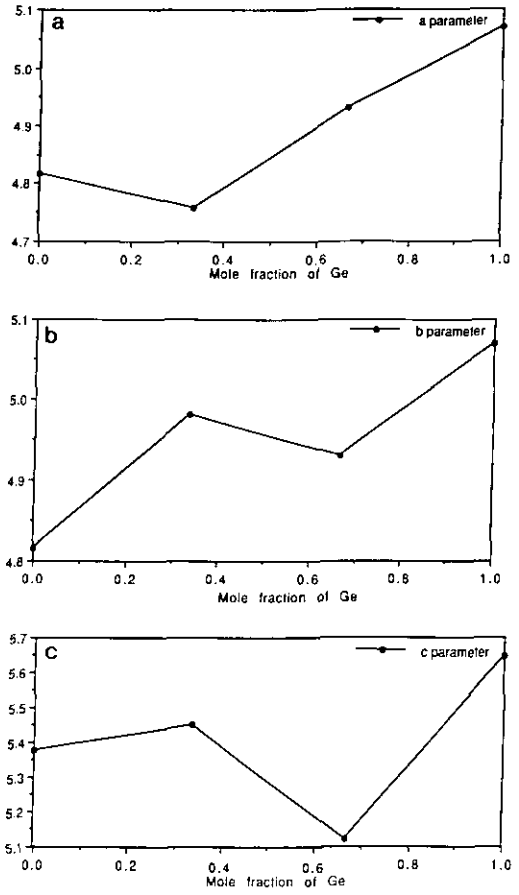

FIG. 3. (a) Lattice parameter *a*, (b) lattice parameter *b*, and (c) lattice parameter *c* vs mole fraction Ge for quartz. (All lattice parameters in Å).

Silicalite-I. Two models of the Ge arrangement have been used to study this structure. The first, is as nearly as possible, a random one, in which Ge and Si are permuted over the T sites in an unbiased way, via a computer generated algorithm. It is of course not possible to generate an entirely random arrangement as our method is based on the use of periodic boundary conditions. However, the large unit cell of silicalite permits an extensive range of distributions. The other model involves location of the Ge ions along the straight channel, thus forming layers of Si and Ge. Figure 4 presents a plot of the mixing energy for such systems. Interestingly, the random structure has the lower energy. A fitted second order polynomial yields a minimum energy close to the 1 : 1 ratio. Figures 5a,b,c show plots of the lattice cell parameter versus mole fraction, which reveal the same nonlinear trend as seen in the quartz type structure. For the random structures, the relationship between the lattice cell parameter and the mole fraction is almost linear and is in agreement with Vegard's law. However, the "ordered" arrangement tends to exhibit positive or negative deviations from the linear relationship, which is in line with their lower stabilities. The *a* and *b* directions both show "negative" deviations from linearity, while the *b* direction reveals a positive deviation. For the *b* parameter, the deviation is at most 1% from the value for the random structure. These results indicate that the cell parameter is sensitive to the arrangement of the two types of atom over the T sites. It is conceivable that kinetic factors could freeze in nonrandom Si/Ge distributions. The present calculations show how such effects could be revealed by accurate lattice parameter measurements.

Recent experimental work has been reported on the formation of Ge rich MFI type zeolites (*18*) and samples as high as a 1 : 1 ratio have been synthesized. Table II makes a comparison with the calculated lattice parameters and the experimental results for the mole fractions experimentally available. The agreement between data for a 17.1% synthesized germanium polymorph and a 16.6% Ge calculated polymorph is excellent with an overall error of less than 0.5%. Some of the accuracy of the simulations is due to error compensation. However, this result supports the realibility of the other calculations of the yet to be synthesized structures. EXAFS studies of these compounds have confirmed that the Ge has fourfold coordination, supporting the presence of Ge in the

TABLE I

A SUMMARY OF THE LATTICE CELL PARAMETERS FOR THE PURE GERMANIC POLYMORPHS*

	Calculated		Experimental (*21*)	Error
α-Quartz				
a	5.0702		4.987	1.668%
b	5.0702		4.987	1.668%
c	5.6460		5.652	0.106%
Silicalite-I				
a	21.254	α 89.44		
b	21.004	β 90.0		
c	14.184	γ 90.0		
Zeolite-Y				
a	18.168	$\alpha = \beta = \gamma = 90.0$		
b	18.168			
c	18.168			
Mordenite				
a	19.088	$\alpha = \beta = \gamma = 90.0$		
b	21.337			
c	7.898			

*Cell lengths/Å; cell angles/°.

framework (*19*). Indeed, our results for the random distribution model are in good agreement with their conclusions, that the lattice parameter increases regularly with Ge content. A calculated bond length of 1.67Å ± 0.02Å is found for 16.6% Ge and 1.67Å ± 0.01Å for 6.2% Ge; compared to experimental values of 1.71Å ± 0.02Å for 8.33% Ge and 1.72Å ± 0.02Å for 16.6% Ge. These experimental results were recorded after calcination, since the structural disorder is found to be lowered after such treatment. For the simulated pure GeO_2 phase of Silicalite-I a bond distance of 1.66 ± 0.01Å is calculated, with O–Si–O angles of 109.47 degrees and Si–O–Si angles in the range of 105–112 degrees; the pure GeO_2 form of Silicalite-I has yet to be made.

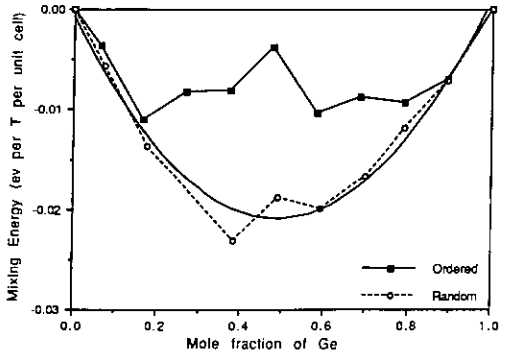

FIG. 4. Mixing energy for a Silicalite-I type structure vs mole fraction of Ge. Equation of fitted curve:

$$y = -7.0468 \times 10^{-4} - 8.2423 \times 10^{-2} x + 8.4149 \times 10^{-2} x^2 \quad (R^2 = 0.969).$$

Zeolite-Y. This is one of the less dense zeolite structures studied and includes large open cavities. We modeled the structure with *F* symmetry and not *P*1 as in the previous simulations, due to the copious number of independent atomic positions in the lower *P*1 cell. Despite these necessary approximations the same trends are evident. Figure 6 shows the variation in the mixing energy with the mole fraction of Ge. One feature evident here is that the "ordered" arrangement is of lower energy than the random structure, in contrast to the results for silicalite-I. Again we find that the properties

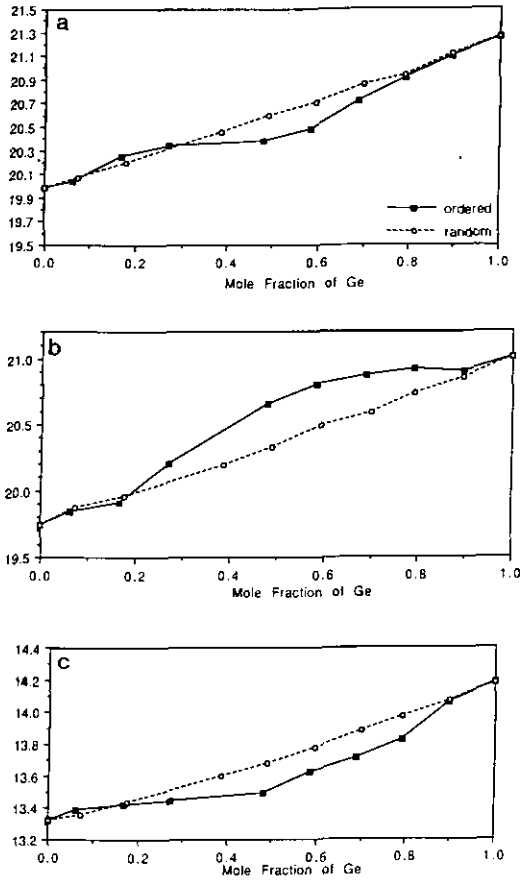

FIG. 5. (a) Lattice parameter a, (b) lattice parameter b, and (c) lattice parameter c vs mole fraction Ge for Silicalite. (All lattice parameters in Å).

are dependent on the arrangement of Si or Ge on the T sites, (Fig. 7a,b,c.) Yet the calculated compositions of minimum energy are similar for both types of distribution.

Mordenite. Mordenite differs significantly from the previous structures due to the presence of four distinct crystallographic sites: T1 and T2 each occupying 16 sites in the unit cell, with T3 and T4 occupying 8 other positions. Therefore we have the opportunity of studying the effect of substitution at distinct crystallographic sites. Figure 8 depicts the now familiar plot for the variation of the heat of mixing with composition, with a second order polynominal fitted to the model based on the random distribution. The composition of the minimum energy structure, obtained by fitting a suitable second order polynominal to the energies for the random arrangements, is close to a 1 : 1 Ge/Si ratio. It is clear that the energetics of substitution of the Ge are strongly dependent on the T site substituted even for the equimolar composition. The largest calculated difference occurs for the 1 : 1 ratio with the value for the random arrangement lying between that for the two ordered arrangements which correspond to the loading of T1T3 and T2T3 sites for which the difference in energy is approximately 4.0 KJ/mole. Substitution at one particular site can alter the energetic properties quite significantly. Figure 9a,b,c describes the variation of the lattice parameter with mole fraction. Both positive and negative deviations from Vegard's Law can be seen. A point to note is that there appears to exist a crossover from negative to positive deviations at around 30% Ge in each case. The effect of substitution at one T site can be dramatically different from those of substitution at another, although the chemical compositions are the same. If Vegard's law applied then the effect should be similar. It would be of particular interest if these predictions could be tested experimentally.

Table I summarizes the calculated and experimental lattice parameters for the pure GeO_2 polymorphs. As regards the calculated energies it is best to relate the results to the quartz type structure allowing a sensible comparison to be made between the purely siliceous and purely germanic forms. Figure 10 presents such a comparison. For GeO_2 the mordenite structure is closer in energy to that of quartz, than is the case for SiO_2. This might have implications for the stability of the pure Ge mordenite phase as compared to the silicalite-I structure. Overall how-

TABLE II

A COMPARISON OF LATTICE PARAMETERS (Å) FOR RANDOM AND ORDERED SUBSTITUTIONS OF Ge IN SILICALITE-I WITH EXPERIMENTAL DATA

Composition	Calculated	Experimental (*21*)		Error
16.6% Ordered		17.1% Ge		
a	13.415	*a*	13.428	0.06%
b	20.256	*b*	20.137	0.59%
c	19.907	*c*	19.939	0.16%
16.6% Random				
a	13.434			0.04%
b	20.1968			0.30%
c	19.958			0.10%

ever, the relative energies of zeolitic GeO_2 polymorphs with respect to that of the quartz structure are broadly similar to those for the SiO_2 zeolitic polymorphs relative to the quartz polymorph of SiO_2.

Experimentally a loading of up to 50% Ge has been achieved for the Silicalite-I structure (*17*), and the experimental structures are in good agreement with the simulations (see Table II,) at the relevant mole fractions. Thus from the calculations and available experimental data it is likely that a fully germanic analogue of Silicalite-I could be synthesized.

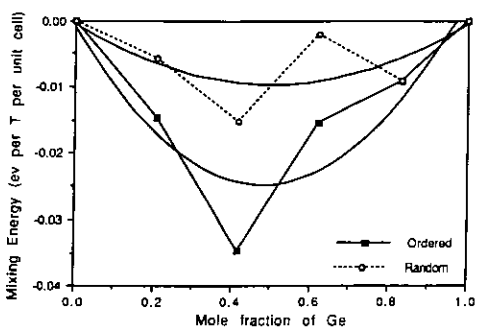

FIG. 6. Mixing energy of a Zeolite-Y type structure vs mole fraction of Ge. Equation of fitted curve RANDOM:

$$y = -4.3599 \times 10^{-4} - 3.7313 \times 10^{-2} x + 3.7245 \times 10^{-2} x^2 \quad (R^2 = 0.453).$$

Equation of fitted curve ORDERED:

$$y = 8.6441 \times 10^{-4} - 9.9878 \times 10^{-2} x + 0.10382 x^2 \quad (R^2 = 0.779).$$

Part 2. Lattice Dynamical Calculations

Calculated spectrum of quartz. Figure 11 depicits the variation in the IR spectra with change of mole fraction of Ge. A comparison of the calculated purely siliceous spectrum with the experimental spectrum has been given previously (*20*). We are mainly interested here in the *variation* of the spectra with mole fraction of Ge and the question of how we might extract quantitative results from such calculations. There is a definite downward shift of the peaks, owing to a weakening of the average T–O bond. But of greater interest is the increase in the activity in the 570–750 cm^{-1} range. In the pure SiO_2 structure, there is little vibrational activity in this area; we predict an increase in the intensity as the Ge content rises.

Calculated spectra of Silicalite-I. Using the code and techniques previously described, the IR spectra can be calculated for all the arrangements of Ge in Silicalite-I. Figure 12 shows these spectra for the random distribution models at differing mole fractions of Ge. As can be seen, there is a gradual change from one spectrum through to the other, but the SiO_2 lattice vibrations remain visible up to approximately 68%, as

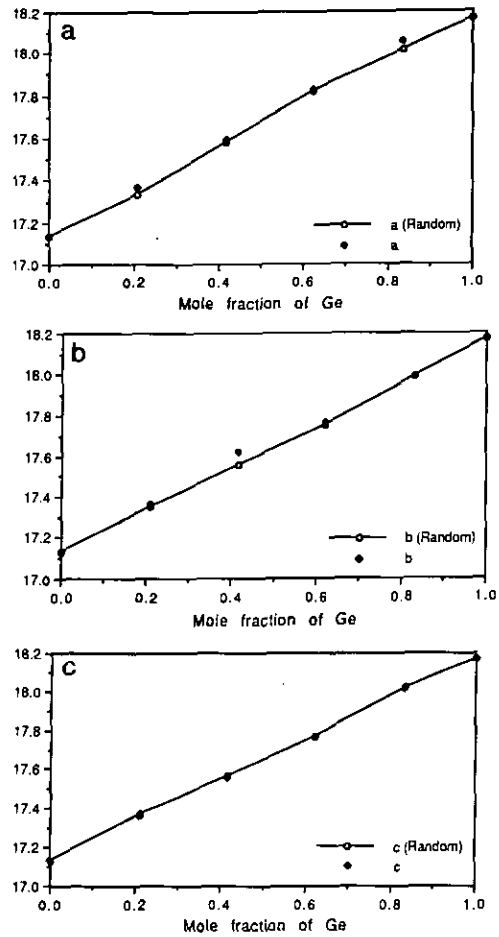

FIG. 7. (a) Lattice parameter a, (b) lattice parameter b, and (c) lattice parameter c vs mole fraction Ge for Zeolite-Y. (All lattice parameters in Å).

in e.g., the T–O asymmetric stretch at 900 cm^{-1}. The GeO_2 lattice vibrations, on the other hand only really take shape after about 60% Ge substitution. Again, there is an overall downward shift due to the weakening of the T–O bonds. On comparing the pure GeO_2 structure and the purely siliceous form a splitting is clearly visible around 400 cm^{-1}. It would be interesting to compare the experimental spectra of the pure polymorphs in order to test these predictions. The spectra of the compounds with an ordered Si/Ge distribution exhibit all the trends that are apparent when considering those for the structures with random arrangements. There are slight differences but again these can be attributed to the high dependence of the vibrational spectra on ion arrangements. Indeed the most notable differences occur around 50% substitution, where there is the greatest number of Si/Ge permutations.

Calculated spectra of Zeolite-Y. The calculated IR spectra are depicted in Fig. 13a,b. The simulated purely siliceous spectrum has previously been compared to an experimental spectrum of a dealuminated compound in de Man *et al.* (*20*) Here we concentrate on the dramatic effect of differing Ge substitutions into the lattice framework. As can be seen the transition from a purely siliceous to a purely germanic form is substantial. When one considers the results for a purely random substitution model, the spectra change from an ordered set of peaks, through a highly diffuse set, to an ordered Ge spectrum. The effect of the Ge substitution is to shift the peaks to

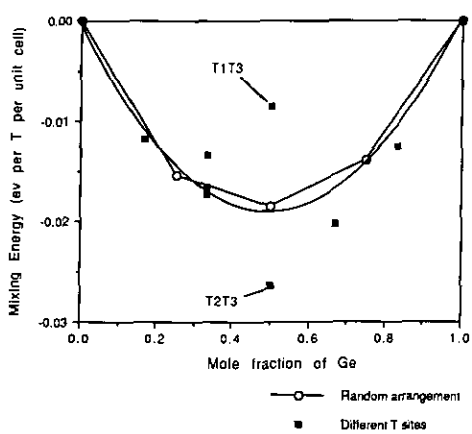

FIG. 8. The mixing energy of a Mordenite type structure vs mole fraction. Equation of the fitted curve:

$$y = -3.8745 \times 10^{-4} - 7.5186 \times 10^{-2} x + 7.5774 \times 10^{-2} x^2 \quad R^2 = 0.995.$$

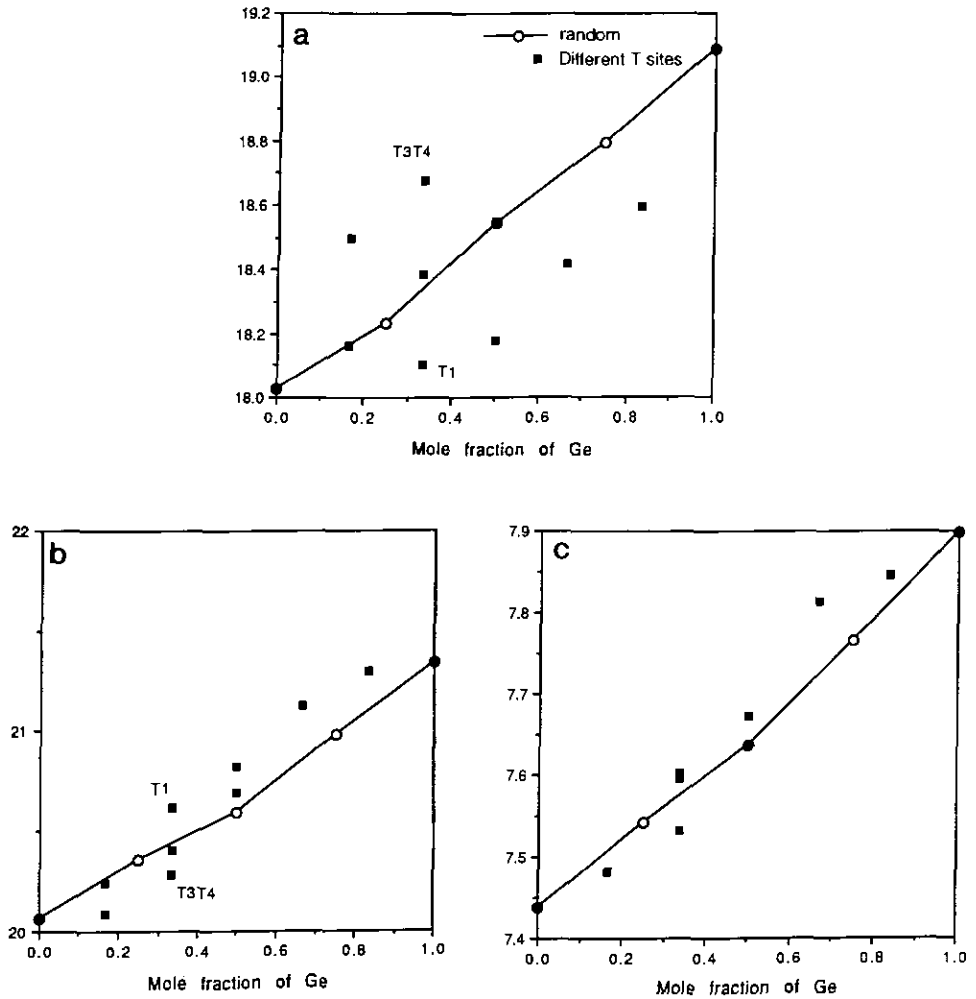

FIG. 9. (a) Lattice parameter a, (b) lattice parameter b, and (c) lattice parameter c vs mole fraction Ge for Mordenite. (Lattice parameters in Å).

a lower frequency owing to the general weakening of the T–O bond.

In the spectra of the ordered structures, the transition is much clearer: the predominant T–O symmetric and asymmetric peaks are removed as the concentration of Ge increases. The effect of introducing Ge into the purely siliceous lattice is somewhat dissimilar to that of including Si into the pure GeO_2 lattice; in the latter case the modification of the spectrum is substantially greater, suggesting the SiO_2 is less perturbed by the introduction of disorder in the T sites than is GeO_2.

It would clearly be of considerable interest to compare these predicted spectra with experimental measurements.

Calculated spectra of Mordenite. Figure 14a shows the calculated IR spectra of the random arrangement of Ge in Mordenite and it clearly demonstrates the transformation of the pure SiO_2 spectrum to a pure GeO_2

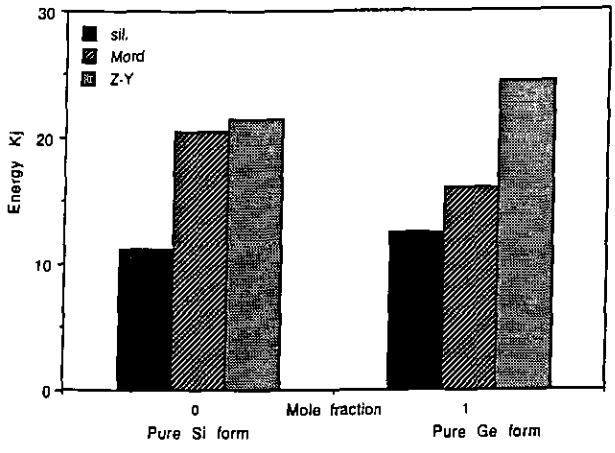

FIG. 10. The relative energies (per mole with respect to the quartz structure) of pure SiO_2 and pure GeO_2 polymorphs.

spectrum. The peak at 375 cm^{-1} is observed to decrease in intensity and reform at a lower wavenumber, which can be attributed to the weakening of the pore modes. The behavior shown in the figure is typical of that for structures with random distributions of Ge substituted into zeolitic structures.

In Fig. 14b the spectra are shown for the substitution of Ge at differing T sites. They are evidently highly varied even though the

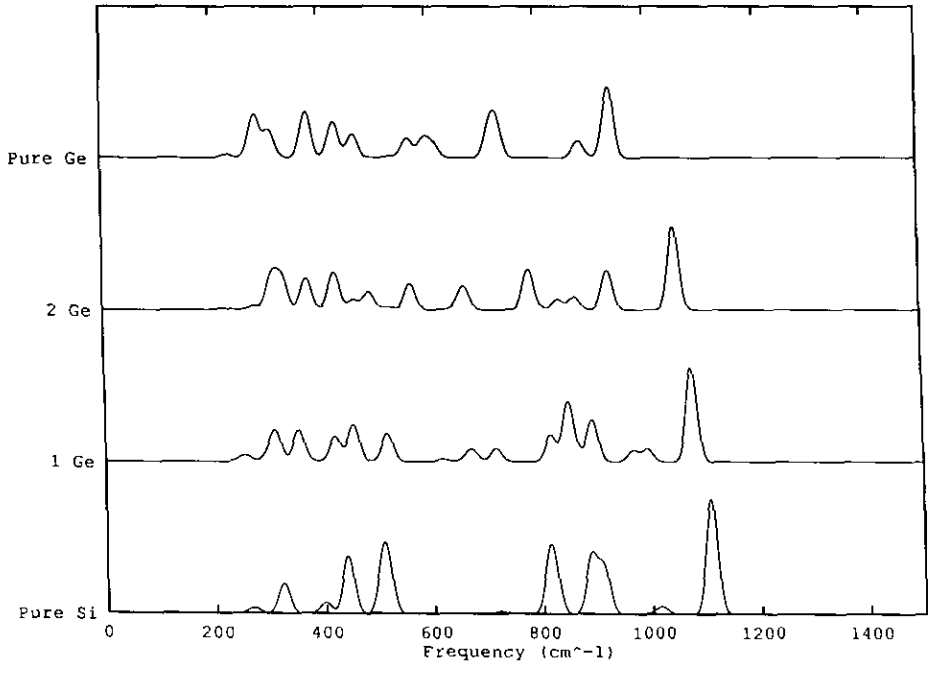

FIG. 11. Predicted IR spectra for Ge substitution in quartz. (All intensities in this and subsequent figures in arbitrary units).

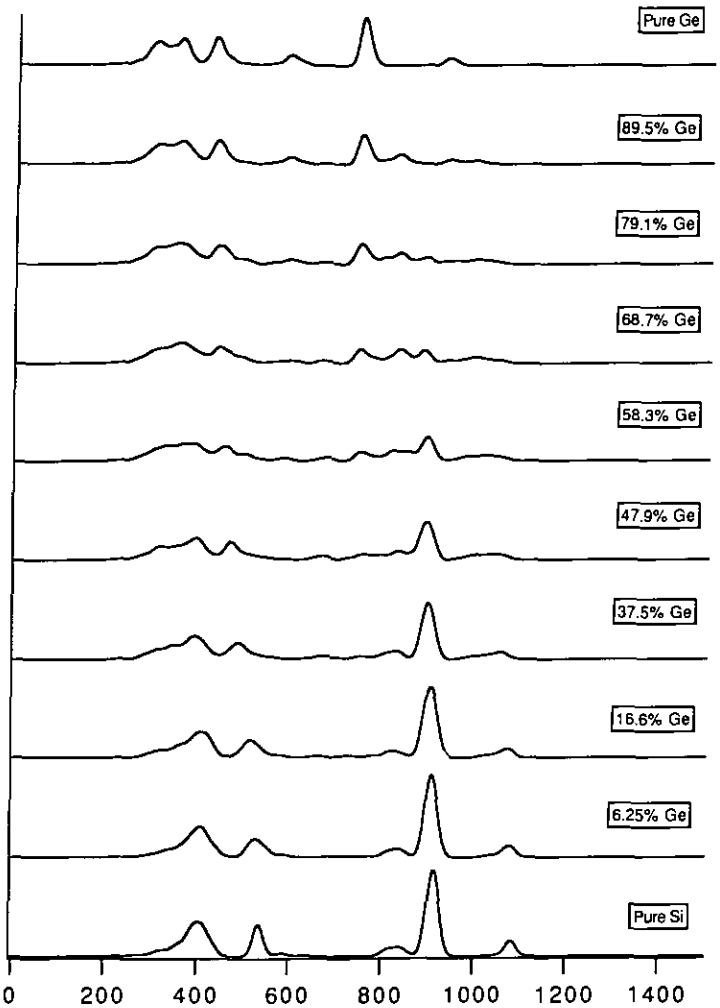

FIG. 12. Predicted IR spectra for RANDOM Ge substitution in Silicalite-I.

mole fraction is constant. For substitution at each site we observe a distinct spectrum which differs markedly from the spectrum for the random structure model of similar mole fraction, where the spectra are less structured. Indeed from "doping" of certain crystallographic sites, one can analyze the importance of specific site substitutions from the spectra. The peak at 1150 cm^{-1} can be attributed to the intra-trahedral asymmetric stretch of the T1 and T2 sites; upon Ge doping of these sites the peak is observed to shift downward, due to T–O bond weakening. However, on substitution of only the T3 and T4 sites, it is still apparent at the frequency previous calculated; indeed, there is a great deal of potential information in this data. The T4 site gives rise to the T–O asymmetric stretch around 1050 cm^{-1}, because upon substitution of all but this site, the peak is still observed in the spectrum and can be compared with the pure Si spectrum since it is not shifted downward. Such independent T–O vibrations and

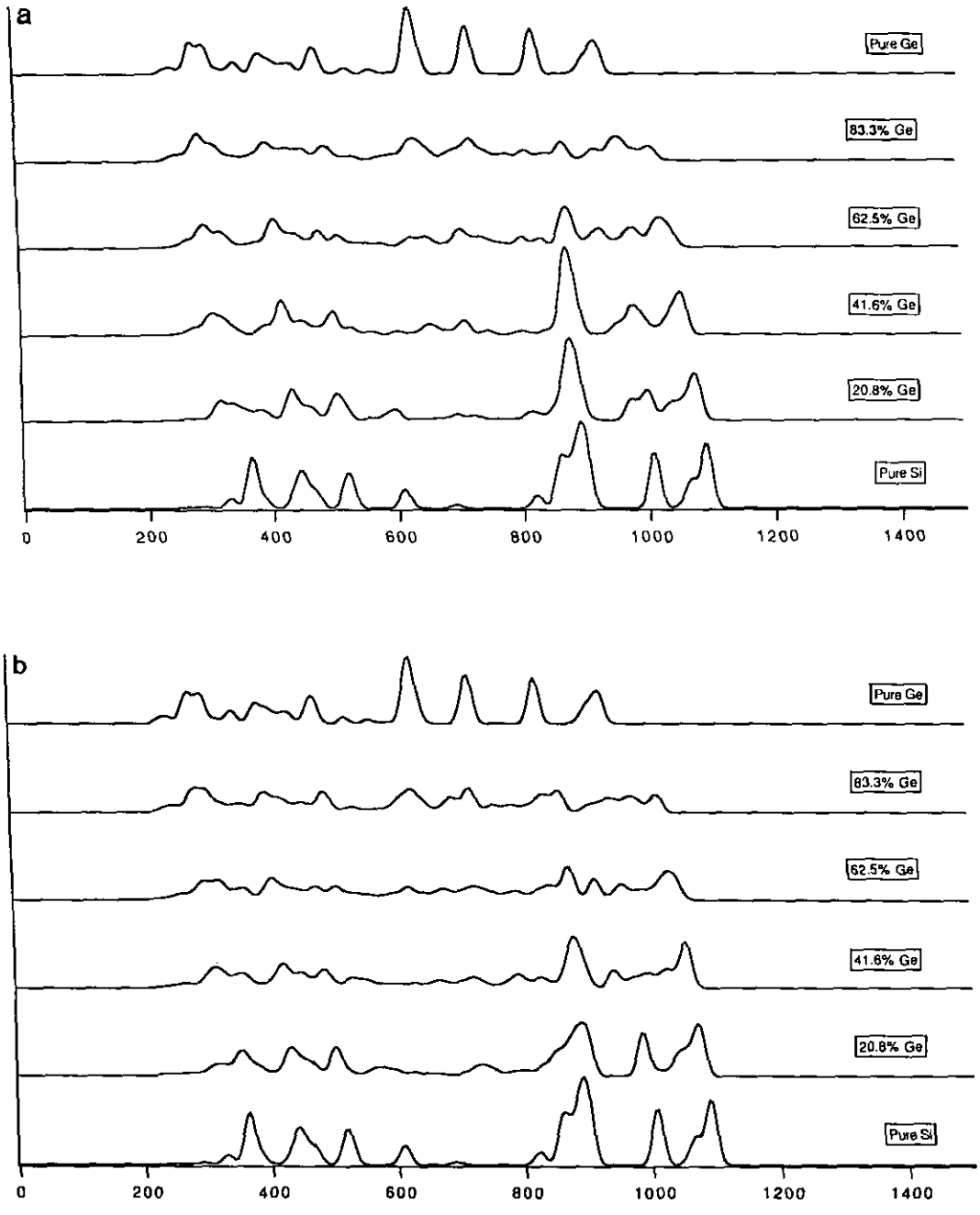

FIG. 13. Predicted IR spectra for (a) ORDERED and (b) RANDOM Ge substitution in Zeolite Y.

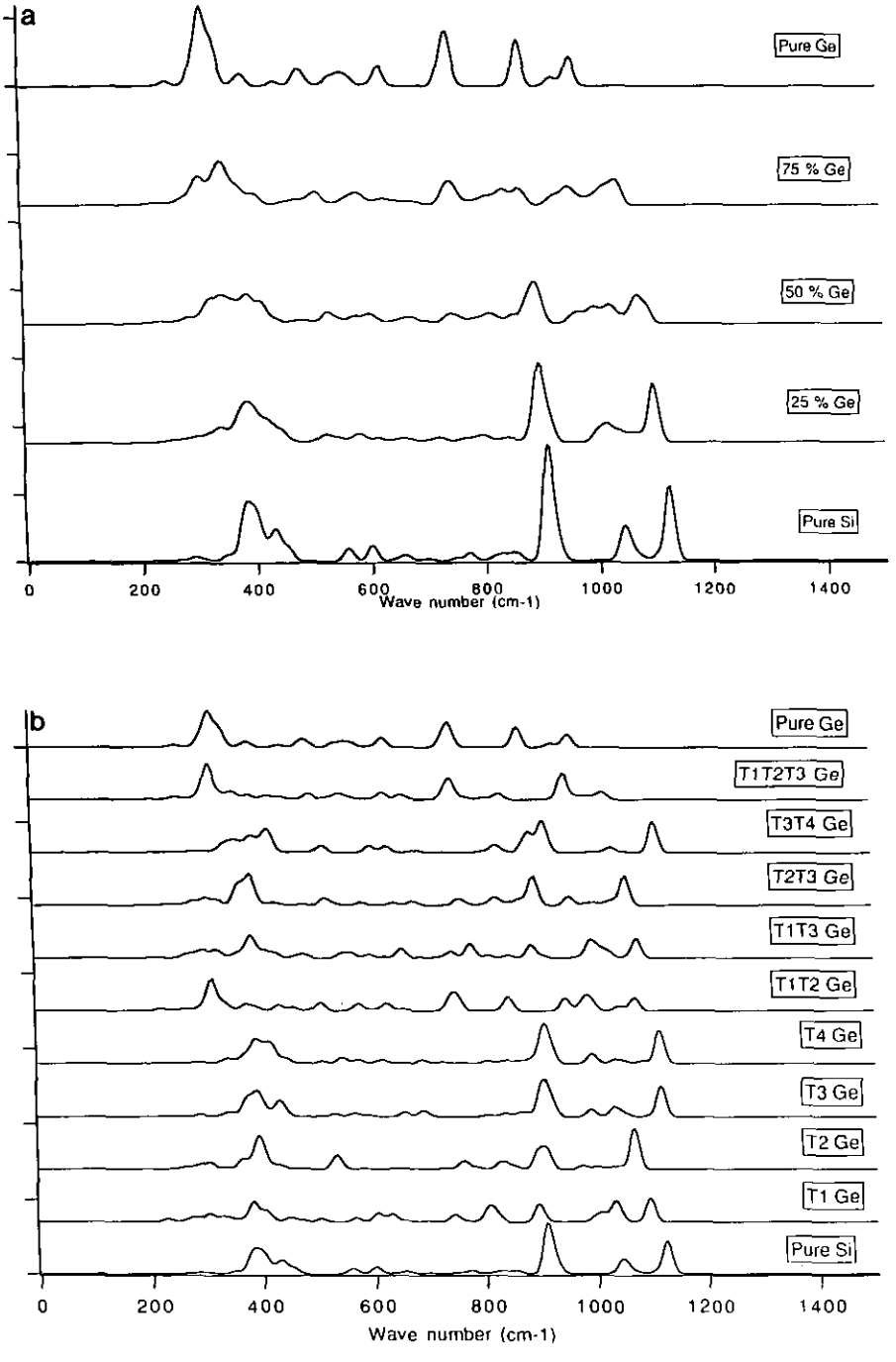

FIG. 14. Predicted IR spectra for (a) RANDOM and (b) ORDERED Ge substitution in Mordenite.

their relative contributions are easily analyzed, but for the pore modes, less than 600 cm^{-1}, a more detailed study is required. One conclusion that can be made is that the 350 cm^{-1} peak is due to enhancement by the T1 and T2 sites upon substitution. Since this peak is not observed when the T1 or T2 sites are substituted independently, but when both sites are substituted, a pore mode vibration of significant intensity is calculated. As can be seen from Fig. 14a a great deal of information is available; much more than is possible for the models based on random arrangements. Once it becomes experimentally possible to create such Ge-containing analogues of Mordenite it will be of great interest to compare calculated and experimental spectra as the IR spectrum is highly dependent upon the arrangement of framework ions.

Conclusion

GeO_2 polymorphs with zeolitic structures are predicted to have roughly the same thermodynamic stabilities with respect to the quartz polymorphs as do corresponding SiO_2 polymorphs. Moreover, complete solid solutions of SiO_2/GeO_2 are predicted within the structures considered in this paper.

Vegard's law is observed (as is expected) when there are random arrangements over the T sites, but not for ordered structures. The large deviations in the calculated lattice cell parameters might provide a method for deducing whether there is order in such zeolite structures.

The variation of the calculated IR spectra with germanium substitution, show marked differences between the random and the ordered form. Indeed these show how the detailed arrangement of framework ions can significantly change the vibrational properties of the solid.

Acknowledgments

We thank the SERC for general support (to JMT and CRAC) and for a quota studentship to ARG.

Appendix A: Potentials Used in This Study

Atomic Parameters

	Core Charge (|e|)	Shell Charge (|e|)	Spring Constant (eV/Å²)
Silicon	4.0	—	—
Germanium	4.0	—	—
Oxygen	0.86902	−2.86902	74.92

Interatomic Buckingham Potential Terms

	A(eV)	ρ(Å)	C(eVÅ⁶)
Silicon–oxygen (shell)	1283.907	0.32052	10.66158
Germanium–oxygen (shell)	1980.02	0.3172	53.66
Oxygen (shell)–oxygen (shell)	22764.0	0.149	27.88

Three-body potential for

O–Si–O : k = 2.09724 eV rad^{-2}; ϑ^0 = 109.47

O–Ge–O : k = 0.5861 eV rad^{-2} ; ϑ^0 = 109.47

References

1. R. M. Barrer, "Zeolites and Clay Minerals," Academic Press, New York (1972).
2. S. Wilson, B. M. Lok, C. A. Menina, T. R. Cannon, and E. M. Flanigen, *J. Am. Chem. Soc.* **104,** 1146 (1982).
3. E. M. Flanigen, B. M. Lok, R. L. Patton, and S. T. Wilson *in* "New Developments in Zeolite Science and Technology" (P.A. Jacobs, Ed.), p. 103, Elsevier, Amsterdam (1985).
4. D. E. W. Vaughan, *Stud Surf. Sci. Catal.* **49A,** 95–116 (1989).
5. P. A. Wright, S. Natarajan, J. M. Thomas, R. G. Bell, P. L. Gai-Boyes, R. H. Jones, and J. Chen, *Angew Chem. Int.* **31,** *(11)* (1992).
6. "Computer Simulation of Solids" (C.R.A. Catlow and W. C. Mackrodt, Eds.), Lecture Notes in Physics, Vol. 166, Springer-Verlag, Berlin, New York.
7. R. A. Jackson and C. R. A. Catlow, *Mol. Simulation* **1,** 207–224 (1988).
8. R. G. Bell, private communication.
9. P. P. Ewald, *Ann. Phys.* (Leipzig) **64,** 253 (1921).
10. M. Leslie, Daresbury Laboratory Technical Memorandum," in preparation.
11. S. Parker and D. Price, *in* "Advances in Solid State Chemistry" (C. R. A. Catlow, Ed.). Vol. 1, p. 295 (1989).

12. S. DOLLING, *in* "Methods in Computational Physics" (G. Gilet, Ed.), Vol. 15 (1976).
13. A. A. MARADUDIN, E. W. MONTROLL, G. H. WEISS, AND I. P. IPATOVA, "Theory of Lattice Dynamics in the Harmonic Approximation Approach," Academic Press, New York (1971).
14. D. A. KLEINMAN AND W. G. SPITZER, *Phys. Rev.* **125,** 16 (1962).
15. A. J. M. DE MAN, PH. D. Thesis, Eindenhoven University, Holland, (1992).
16. A. MIEIZNIKOWSKI AND J. HANUJA, *Zeolites* **7,** 249 (1987).
17. B. HOUSER, N. ALBERDING, R. INGALLS, AND E. D. CROZIER *Phys. Rev. B.* **37,** 6513 (1988).
18. Z. GABELICA AND J. L. GUTH, "Zeolites: Facts, Figures, Future" (P. A. Jacobs and R. A. van Santen, Eds.), Elsevier, Amsterdam (1989).
19. M. H. TUILIER, A. LOPEZ, J. L. GUTH, AND H. KESSLER *Zeolites* **11,** 662–665 (1991).
20. A. J. D. DE MAN, B. W. H. VAN BEEST, M. LESLIE, AND R. A. VAN SANTEN, *J. Phys. Chem.* **94,** 2524 (1990).
21. G. S. SMITH AND P. B. ISAACS, *Acta Crystallogr.* **17,** 842 (1964).